J Electroceram
DOI 10.1007/s10832-012-9777-5

Photoluminescence and optical dispersion parameters of N-doped ZnO nano-fiber thin films

M. S. Abd El-saddek · I. S. Yahia · Z. A. Alahmed · F. Yakuphanoglu

Received: 17 September 2012 / Accepted: 11 December 2012

Abstract N-doped ZnO (NZO) nanocrystalline thin films were successfully synthesized via sol–gel method. The structural and optical properties of the films were characterized by various techniques including X-ray diffraction, atomic force microscopy (AFM), UV–vis absorption and photoluminescence. The UV–vis absorption edge was changed with increasing N-doping concentration. X-ray diffraction (XRD) results clearly showed that the zinc oxide doped with nitrogen (5 to 20 wt.%) were identified with phases of hexagonal ZnO and N-doped ZnO nanocrystalline thin films. The refractive index dispersion mechanism obeys the Single oscillator model. The dispersion parameters E_o and E_d of the thin films were determined. The dispersion parameters were changed by N dopant. It is evaluated that the structural, optical constants, photoluminescence properties of Zinc oxide film can be controlled by N dopants.

M. S. Abd El-saddek (✉)
Nanomaterials Laboratory, Physics Department,
Faculty of Science, South Valley University, Qena 83523, Egypt
e-mail: el_sadek_99@yahoo.com

M. S. Abd El-saddek
e-mail: mahmoud.abdelsadek@sci.svu.edu.eg

I. S. Yahia
Nano-Science&Semiconductor Labs., Physics Department,
Faculty of Education, Ain Shams University, Cairo, Egypt

I. S. Yahia
Department of Physics, Faculty of Science, King Khalid
University, P.O. Box 9004, Abha, Kingdom of Saudi Arabia

Z. A. Alahmed
Department of Physics and Astronomy, College of Science,
King Saud University, Riyadh 11451, Kingdom of Saudi Arabia

F. Yakuphanoglu
Department of Physics, Faculty of Science, Firat University,
Elaziğ, Turkey

Published online: 28 December 2012

Keywords ZnO nanocrystalline · N-doped ZnO · Sol–gel calcinations method · Spin coating · Optical properties · Photoluminescence spectroscopy

1 Introduction

ZnO is a wide band gap semiconductor and has received a particular attention owing to its promising applications, such as piezoelectric devices, gas sensors, thin film transistors, surface acoustic wave devices, and transparent electrodes for thin film solar cells [1, 2]. Furthermore, the ZnO film is also known to be a material for blue or ultraviolet emitting devices [3].

For applications of transparent and conducting electrode in solar cells and thin-film transistor, the development of low-resistive ZnO films with high transparency is important [4]. Due to its large exciton binding energy (60 meV), wide band gap (3.37 eV) and facilitate synthesis and assembly methods, the utilization of ZnO has covered various fields such as electric transistors [5], photovoltaic devices [6] and chemical sensors [7]. Physical properties of undoped and doped ZnO films have been widely reported. In spite of extensive studies on preparation, characterization and the effect of doping on the properties of ZnO, certain effects of either some dopant or preparation procedures are still remaining unclear. There have been several reports on the growth of n-type ZnO doped with group III elements such as Al, Ga, and In [8–10]. One of the major obstacles in the development of ZnO-based optoelectronic devices is to realize an efficient p-type doping. Great efforts have been made to obtain p-type ZnO films using an acceptor dopant such as N, As, and P. However, As and P are deep acceptors and don't contribute significantly to p-type conduction [11]. Recently, N has proven to be a suitable acceptor for making p-type ZnO [12], and N-doped ZnO (ZnO:N) has been fabricated by various deposition methods [13–16].

Various methods have been used to prepare p-type ZnO thin films including chemical vapor deposition (CVD), sputtering, spray deposition, and oxidation of Zn_3N_2. Compared with the above methods, sol–gel method is a simple, safe, non-vacuum method, and low cost method to prepare ZnO materials compared with conventional synthesis method such as magnetic sputtering, chemical vapor deposition, and hydrothermal reaction [17]. Moreover, it is easy to realize dopant incorporation using a one-route process simply by modulating the ingredient of the precursors. Our work is continuing on the synthesis and characterization of metal oxide nanomaterials, especially ZnO and CdO doped with different metals to standup their characterization for the advanced technological applications [18, 19].

In general, unintentionally doped ZnO is of n-type conduction due to the presence of native donor-like defects. Up to now, the reliable and reproducible realization of p-type ZnO is still a great challenge [20–24]. Different dopants have been employed to realize p-type conductivity [21–23], and among these dopants, nitrogen is the most attractive candidate according to theoretical calculations and experimental observations [24, 25].

In the present work, N-doped ZnO nanocrystalline thin films have been synthesized by sol–gel method. The structure, morphology and optical properties of the N-doped ZnO (NZO) have been characterized by means of XRD, AFM, UV-visible and photoluminescence spectroscopy.

2 Experimental details

2.1 Samples preparation

The nanocrystalline samples of ZnO and nitrogen-doped ZnO films were synthesized by sol–gel which was reported in our previous work [26, 27]. The nitrogen-doped zinc oxide films (NZO) were prepared using 0.1 M zinc acetate dehydrate ($(ZnCH_3COO)_2.2H_2O$) and 0.1 M ammonium acetate $(CH_3COO)NH_4$ and 0.1 M 2-methoxyethanol as a solvent. Firstly, the appropriate amounts of zinc acetate dehydrate ($(ZnCH_3COO)_2.2H_2O$) and ammonium acetate (CH_3COONH_4) were dissolved in 2-methoxyethanol at a constant magnetic stirring for 10 min and then, 0.1 M monoethanolamine as stabilizer was added to the solution during the stirring and the solution was stirred constantly for 2 h at 60 °C. The ZnO precursor containing N-dopants were prepared with different percents (5, 10, 15 and 20 %) ammonium acetate. The films of N doped ZnO were deposited using a spin coater with 1000 rpm for five successive layers on glass substrates. After each layer coating, it was dried at 120 °C in air for 10 min. The obtained solid films were annealed at 450 °C for 1 h to remove the organic residual compounds.

2.2 Characterization

The structural properties were determined by X–ray diffraction (XRD) using a D8 BRUKER X–Ray diffractometer with CuK_α radiations (λ=1.54059 Å). The structural properties of the nanocrystalline thin films samples were investigated by Park System XE-100E atomic force microscopy (AFM). Also, the thickness of the undoped and Al doped CdO film was determined by using atomic force microscopy. The optical transmittance, absorbance and reflecatnce spectra in the wavelength of 300–700 nm was recorded using a Shimadzu UV–VIS-NIR 3600 spectrophotometer using an integrating sphere attachment. The photoluminescence (PL) spectra of the prepared films were recorded by a fluorescence spectrophotometer (LS 45) with an excitation wavelength of 325 nm. Electrical conductivity type was measured by hot probe and thermoelectric power measurements (Keithley nanovoltmeter).

2.3 Methodology of the optical constant calculations

The optical constants the refractive index (n) and the absorption index (k) of thin films at different wavelengths, based on an absorbing thin film on a transparent substrate has several orders of magnitude larger than the thickness of the film, the spectrophotometric measurements of transmittance and reflectance measurements were used [28]. Thin films of N-doped ZnO were deposited onto glass substrates are considered to be a homogeneous film. If the film thickness is d and a complex refractive index is given by $\widetilde{n} = n - ik$, where n is the refractive index and k is the extinction coefficient [28].

Following the analysis given by Moss [29], the absorption coefficient α was computed from the experimental measurements of the transmittance $T(\lambda)$ and reflectance $R(\lambda)$ according to the following equation [29]:

$$T = \left(\frac{(1-R)^2 \exp(-\alpha d)}{(1-R)^2 \exp(-2\alpha d)} \right), \tag{1}$$

The reflectance (R) as a function of the refractive index n and the absorption index k is given by the Fresnel formula as [28–32]:

$$R = \left(\frac{(n-1)^2 + k^2}{(n-1)^2 - k^2} \right), \tag{2}$$

where $k = \alpha\lambda/4\pi$. If one solves Eq. 2 via elementary algebraic manipulation, refractive index can be obtained as [28–32]:

$$n = \left(\frac{1+R}{1-R} \right) + \sqrt{\frac{4R}{(1-R)^2} - k^2}, \tag{3}$$

When the film thickness is known, then the computation can be carried out and the optical constants can be calculated.

3 Results and discussion

3.1 Structure and morphology of (NZO) nanocrystalline films

Figure 1 shows the XRD spectra of (NZO) nanocrystalline thin films. All data were smoothed and background subtracted. It indicates that, all the films are crystalline and exhibit the hexagonal structure phase (JCDPS card No.89-1397) [33] in good agreement with pervious data [34]. Three important peaks appear in the recorded range indexed as (100), (002) and (101) planes of a standard wurtzite zinc oxide crystal and the other planes such as (102), (110), (103) and (112) were also visible. The strong and sharp reflection peaks suggested that the as-synthesized (NZO) were well crystallized. There was no other crystalline phase in all of these X-ray diffraction patterns, which indicated that nitrogen atom brings into the crystal lattice of zinc oxide to substitute for oxygen atom and did not bring about a new object phase, which was consistent with the traditional doping theory.

In order to determine the content of the N incorporated in ZnO, the EDX measurement was done on N doped ZnO film. The obtained results for 5 %N doped ZnO film were found to be 1.08 w% for N, 9.60 w% for O, 17.10 w% for Zn and 72.22 w% for Si. This result confirms the content of the N incorporated in ZnO.

Atomic Force Microscopy (AFM) was used for structural characterization in non-contact mode. AFM offers the significant advantage of probing in high details; the surface topography qualitatively (by surface images) and quantitatively (by mathematical quantities like surface roughness) due to its nanometer-scale spatial resolution, both lateral and vertical. AFM has proved to be very helpful for the determination and verification of various morphological features and parameters. The 2D (40×40 μm^2, 5×5 μm^2) and 3D (5×5 μm^2) AFM images of N-doped ZnO nanocrystalline films are shown in Fig. 2(a-e). As seen in Fig. 2(a-e), the ZnO films are formed from fibers. The distribution of the fibers on substrate is changed with N dopants. The diameters of the fibers were determined by XEI park system software and are given in Table 1. The fiber diameter of N doped ZnO films is decreased with respect to undoped ZnO sample and the lowest fiber diameter was observed for 15%N doped ZnO film. The diameter of fibers is of order of nanoscale. This suggests that N doped ZnO films are the nanostructure materials. The electrical conductivity type of the films is measured by hot probe and thermoelectric power measurements. These results indicate that the dominating transport carrier of the film was found to be a hole (p-type).

3.2 Optical properties of NZO nanocrystalline films

Figure 3(a) represents the plots of the transmittance spectra of the undoped ZnO and ZNO nanocrystalline thin films in the range of 300–700 nm. For the longer wavelengths (l>400 nm), all thin films become transparent and no light is scattered or absorbed as non-absorbing region. At shorter wavelengths, (λ<400 nm) known as absorbing region is due to the existence of absorption. The average transmittance in the visible region was observed about 85 % for the studied films. This is important for applications such as transparent

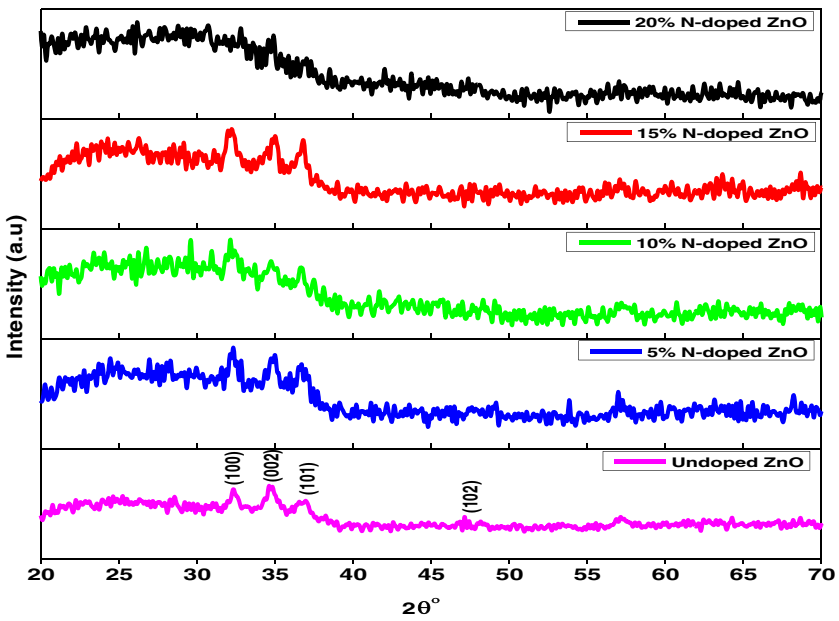

Fig. 1 XRD patterns of ZnO and NZO nanocrystalline thin films

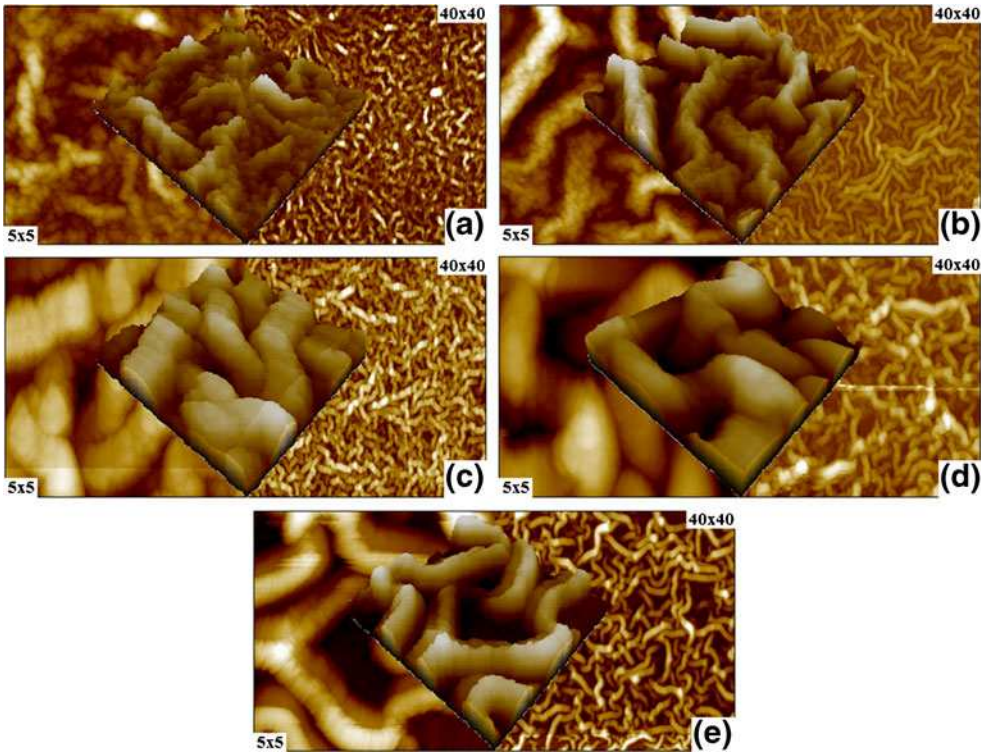

Fig. 2 (**a**-**e**) 2D and 3D AFM images of ZnO samples with different N doping ratios: (**a**) undoped, (**b**) 5 %, (**c**) 10 %, (**d**) 15 % and (**e**) 20 %

conductive films for solar cell windows and various opto-electronic devices. It is clear that weak fluctuation in the spectra is mainly due to interference phenomenon between thin film layers. The average transmittance values are decreased with increasing N dopants. The prepared NZO nanocrystalline thin films showed an increasing absorption near the band edge, which is typical of the transparent conducting oxide films. UV-visible absorption spectra was measured and plotted in Fig. 3(b). As clearly seen in the of Fig. 3(a), the UV absorption edge was red-shifted with increasing the doping concentration, indicating a change in the band gap. It is expected that the change of the band gap of ZnO doped with N is due to an increase of the carrier concentrations which lead to the Burstein–Moss effect [35]. The shift in the optical band gap of any material, usually semiconductors, due to doping effect is known as Bursteing-Moss shift.

Table 1 The calculated mean values of the nano-clusters sizes and the roughness of undoped ZnO and N doped ZnO samples

Samples	Diameter of fibes 5×5, μm^2	Roughness	
		40×40, μm^2	5×5, μm^2
Undoped ZnO	280.151 nm	51.115	50.275
5 %N doped ZnO	185.316 nm	92.303	58.104
10 %N doped ZnO	178.500 nm	80.853	79.219
15 %N doped ZnO	171.872 nm	210.004	147.284
20 %N doped ZnO	185.704 nm	147.802	124.815

The analysis of the dependence of absorption coefficient on photon energy in the high absorption regions is carried out to obtain the detailed information about the energy band gaps. The optical band gap of samples can then be determined by the following relation [36]:

$$(\alpha h\nu)^2 = A\left(h\nu - E_g\right), \tag{4}$$

where A is a constant and E_g is the optical band gap, h is Planck's constant, and ν is the frequency of the incident photon. The optical band gap values of the films were determined from the plots of $(\alpha h\upsilon)^2$ as a function of photo energy $h\upsilon$, as shown in Fig. 3(c). Extrapolating the linear portions of these plots to the x-axis (photon energy) i.e., $h\upsilon$=0, values of E_g for pure ZnO and NZO nanocrystalline thin films were obtained as given in Table. 2. It is seen that E_g values change with nitrogen contents. The shifting in the optical band gaps of the films may be attributed to the band shrinkage effect because of increasing carrier concentration [37–39]. The values of the optical band gap are in good agreement with the previous reported data for the studied samples [34].

Furthermore, the refractive index (n) is a significant factor in optical communication and in designing devices for spectral dispersion and the refractive index dispersion data below the interband absorption edge are important for technological applications of the optical materials, because, the dispersion energy is related to the optical transition strengths and optical conductivity [40]. Values of the refractive index n for the studied N-doped ZnO samples were

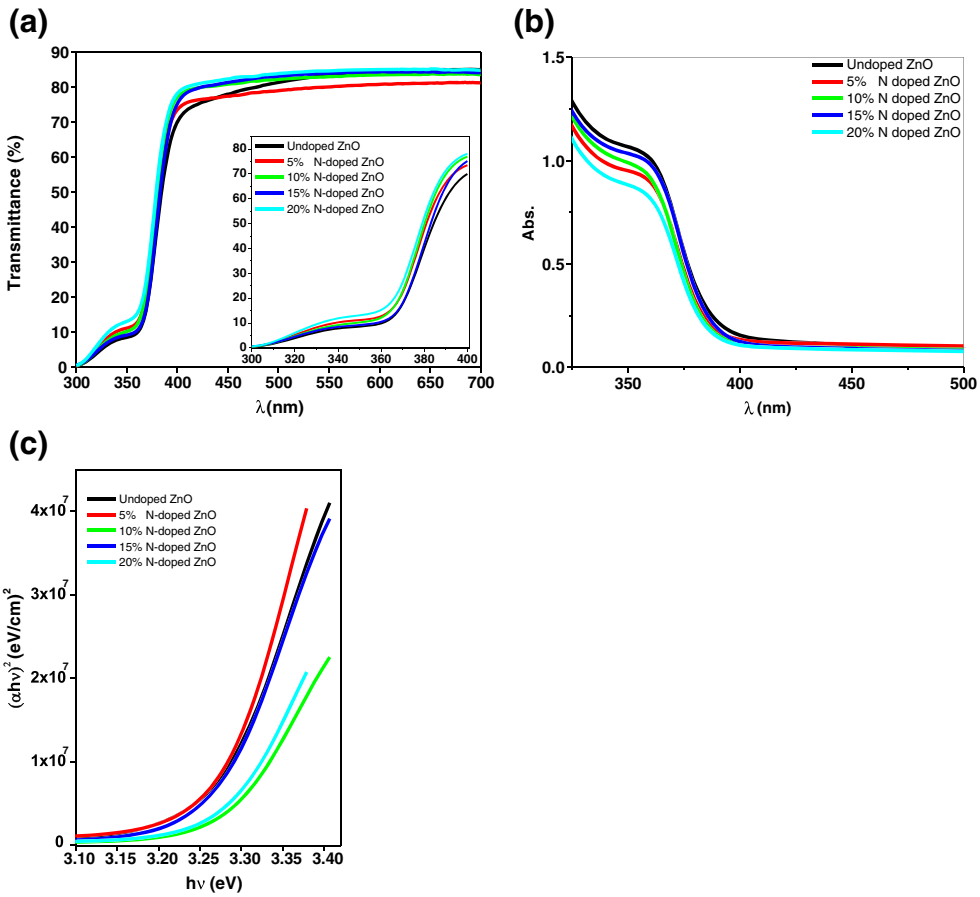

Fig. 3 (**a**) Optical transmittance as a function of wavelengths for undoped ZnO and NZO nanocrystalline thin films at various doping concentrations. (**b**) Optical absorbance as a function of wavelengths for undoped ZnO and NZO nanocrystalline thin films at various doping concentrations. (**c**) Plotting of $(\alpha h\nu)^2$ versus $h\nu$ for undoped ZnO and NZO nanocrystalline thin films at various doping concentrations

calculated based on Eq. 3 i.e., The absorption index k and the reflectance at different wavelengths. The measured reflectance for undoped ZnO and NZO nano-crystalline thin films are shown in Fig. 4. Inset of Fig. 4 shows the variation of refractive index with wavelength for undoped ZnO and NZO nanocrystalline thin films. It is observed that the refractive index n increases up to 400 nm with increasing wavelength and at almost 400 nm, the curve exhibits a peak, after that the refractive index started to decrease with further increase of the wavelengths. It is observed that the values of the refractive index n do not follow a certain trend with increasing N dopants.

Table 2 Optical band gap E_g of undoped and NZO nanocrystalline thin films

Samples	Optical band gap		
	E_g, (eV)	E_o (eV)	E_d (eV)
Undoped ZnO	3.260	4.569	8.753
%5 N doped ZnO	3.267	4.994	7.416
%10 N doped ZnO	3.275	5.903	9.411
%15 N doped ZnO	3.264	5.132	9.279
%20 N doped ZnO	3.279	6.785	10.785

In order to analyze the refractive index dispersion of the films, we used the single-oscillator model, developed by DiDomenico and Wemple [41]. In terms of the dispersion energy E_d and single-oscillator energy E_o, the refractive index at a frequency can be expressed. The single-oscillator model for the refractive index dispersion is expressed as follows [40, 41]:

$$n^2(\omega) = 1 + \frac{E_o E_d}{E_o^2 - (h\upsilon)^2} \tag{5}$$

where n is the refractive index, h is Planck's constant, υ is the frequency, $h\upsilon$ is the photon energy, E_o is the single-oscillator energy for electronic transitions and E_d is the dispersion energy, which is a measure of the strength of interband optical transitions. These parameters can be easily obtained by plotting of $(n^2-1)^{-1}$ versus $(h\upsilon)^2$. The dependence of $(n^2-1)^{-1}$ vs. $(h\upsilon)^2$ at various N-doping contents is given in Fig. 5. The E_d and E_o values were calculated from the slope $(E_d E_o)^{-1}$ and the intercept (E_o/E_d) which is depicted in Fig. 5. It is observed that the values of E_d and E_o do not follow a certain trend with increasing of dopant concentration and the obtained E_d and E_o values suggest that the single-oscillator model is valid for undoped ZnO and ZNO nanocrystalline thin films.

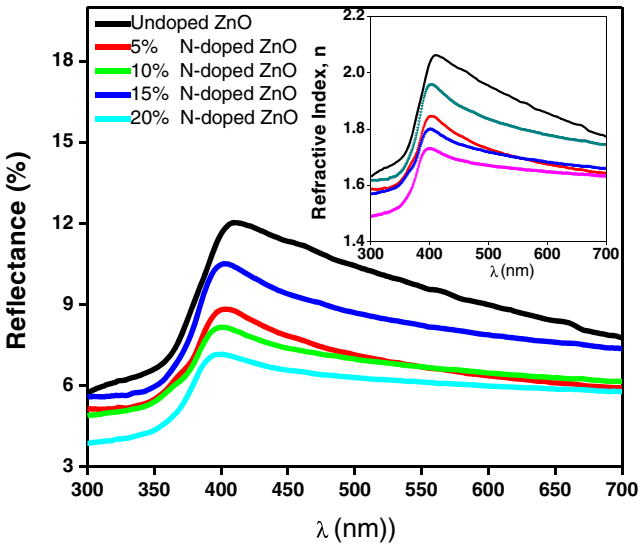

Fig. 4 The variation of the reflectance spectra and refractive index (Inset figure) of with wavelength of NZO nanocrystalline thin films at various doping concentrations

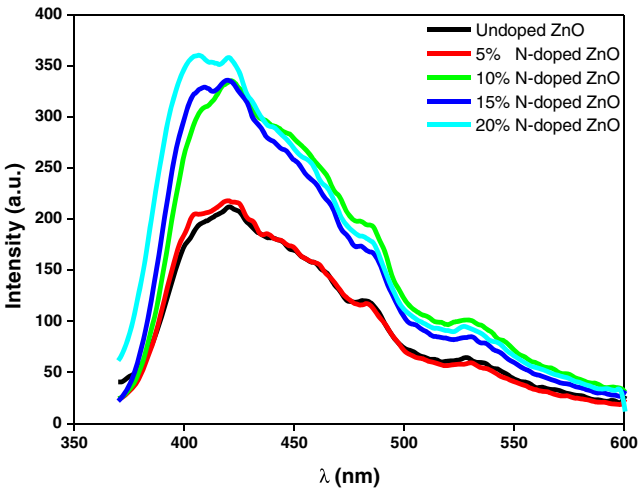

Fig. 6 Photoluminescence spectra as a function of wavelengths for undoped ZnO and NZO nanocrystalline thin films at various doping concentrations

Photoluminescence (PL) measurements were performed for undoped ZnO and NZO films, as shown in Fig. 6. PL measurements were carried out at room temperature to study the luminescent properties of for undoped ZnO and NZO thin films. Two sharp emission bands were observed in the spectra: a first peak at around 406 nm and another emission peak around 420 nm, after this region the PL spectra are decreased as broad green emission band ranging from 485 to 550 nm. The nearly broad band peak at about 404 nm is attributed to the band-to-band transition [42]. The emission peaks at UV region not present in our samples as recorded before for undoped ZnO and NZO, which may attribute to the microstructure change of the investigated samples. It is well understood that PL spectra depend on the stoichiometry and the microstructure of films. The high-energy UV peak was slightly red-shifted and the emission intensity is increased with increasing doping concentration from 5 to 20 %. Further, the green emission was enhanced and red-shifted was changed with increasing doping concentration from 5 to 20 %. The emission band at around 406 nm is attributed to the free exciton emission [43, 44]. The green emission can be explained as the radiative recombination of photo-generated holes with the electrons at the singly ionized intrinsic oxygen vacancies that are ready to form at a high temperature growth [45, 46].

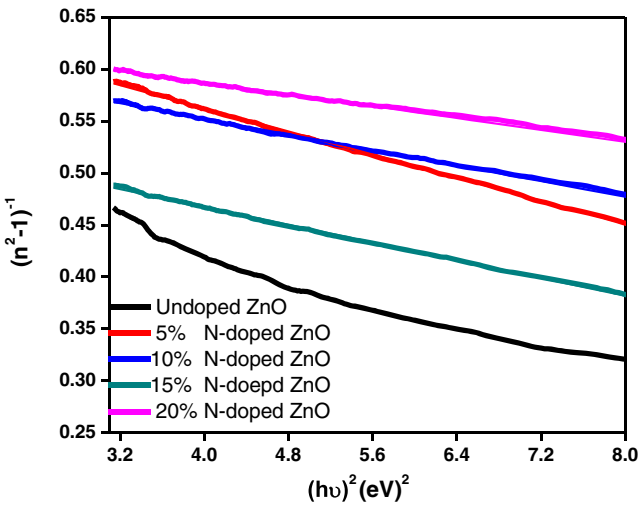

Fig. 5 The plots of of $(n^2-1)^{-1}$ versus $(h\upsilon)^2$ for undoped ZnO and NZO nanocrystalline thin films at various N dopants

4 Conclusions

Undoped and N-doped ZnO nanocrystalline materials were synthesized by sol–gel method. The effects of nitrogen concentration on the surface morphology, structure and optical properties of the doped ZnO were investigated. X-ray diffraction (XRD) results clearly showed that the samples of zinc oxide doped with N (5 to 20 wt.%) were identified with phases of hexagonal ZnO. The optical band gaps of undoped and N-doped ZnO samples were calculated from the plots of $(\alpha h\upsilon)^2$ vs. $h\upsilon$. The optical band gaps of N-doped ZnO samples are changed strongly with N dopants. The band gap energies were changed than the pure ZnO due to Burstein-Moss effect. The optical band and refractive index dispersion parameters E_o and E_d were changed with the dopants concentration. The obtained results suggest that the structural, optical constants, photoluminescence properties of zinc oxide film can be controlled by N dopants.

References

1. Y.-J. Lin, C.-L. Tsai, Y.-M. Lu, C.-J. Liu, J. Appl. Phys. **99**, 063501 (2006)
2. V. Srikant, D.R. Clarke, J. Appl. Phys. **81**(9), 6357 (1997)
3. Y. Zhao, Z. Li, Z. Lv, X. Liang, J. Min, L. Wang, Y. Shi, Mater. Res. Bull. **45**, 1046 (2010)
4. H.Y. Xu, Y.C. Liu, R. Mu, C.L. Shao, Y.M. Lu, D.Z. Shen, X.W. Fan, Appl. Phys. Lett. **86**, 123107 (2005)
5. Y.W. Heo, L.C. Tien, Y. Kwon et al., Appl. Phys. Lett. **85**, 2274 (2004)
6. M. Law, L.E. Greene, J.C. Johnson, R. Saykally, P. Yang, Nat. Mater. **4**, 455 (2005)
7. J. Xu, Q. Pan, Y. Shun, Z. Tian, Sensors Actuators B Chem. **66**, 277 (2000)
8. P. Nunes, E. Fortunato, P. Tonello, F. Braz, P. Vilarinho, R. Martins, Vacuum **64**, 281 (2002)
9. Y. Morinaga, K. Sakuragi, N. Fujimura, T. Ito, J Cryst Growth **174**, 691 (1997)
10. A. Tiburcio-Silver, J.C. Joubert, M. Laveau, Thin Solid Films **197**, 195 (1991)
11. L.G. Wang, A. Zunger, Phys. Rev. Lett. **90**, 1 (2003)
12. A. Kobayashi, O.F. Sankey, J.D. Dow, Phys. Rev. B **28**, 946 (1983)
13. G. Du, Y. Ma, Y. Zhang, T. Yang, Appl. Phys. Lett. **87**, 213103 (2005)
14. L. Chen, J. Lu, Z. Ye, Y. Lin, B. Zhao, Y. Ye, J. Li, L. Zhu, Appl. Phys. Lett. **87**, 252106 (2005)
15. Y. Nakano, T. Morikawa, T. Ohwaki, Y. Taga, Appl. Phys. Lett. **88**, 172103 (2006)
16. Y.J. Zeng, Z.Z. Ye, W.Z. Xu, B. Liu, Y. Che, L.P. Zhu, B.H. Zhao, Mater. Lett. **61**, 41 (2007)
17. J. Lü, K. Huang, J. Zhu et al., Phys. B Condens. Matter **405**, 3167 (2010)
18. R.K. Gupta, F. Yakuphanoglu, F.M. Amanullah, Physica E **43**, 1666 (2011)
19. A.A.M. Farag, M. Cavaş, F. Yakuphanoglu, F.M. Amanullah, J. Alloy Comp. **509**, 7900 (2011)
20. J.F. Rommeluere, L. Svob, F. Jomard, J. Mimila-Arroyo, A. Lusson, V. Sallet, Y. Marfaing, Appl. Phys. Lett. **83**, 287 (2003)
21. T.M. Barnes, K. Olson, C.A. Wolden, Appl. Phys. Lett. **86**, 112112 (2005)
22. F.X. Xiu, Z. Yang, L.J. Mandalapu, D.T. Zhao, J.L. Liu, W.P. Beyermann, Appl. Phys. Lett. **87**, 152101 (2005)
23. K.K. Kim, H.S. Kim, D.K. Huang, J.H. Lim, S.J. Park, Appl. Phys. Lett. **83**, 63 (2003)
24. C.H. Park, S.B. Zhang, S.H. Wei, Phys. Rev. B **66**, 073202 (2002)
25. W. Liu, S.L. Gu, J.D. Ye, S.M. Zhu, Y.X. Wu, Z.P. Shan, R. Zhang, Y.D. Zheng, S.F. Choy, G.Q. Lo, X.W. Sun, J. Crystal Growth **310**, 3448 (2008)
26. Z. Wu, Z. Bao, L. Cao, C. Liu, Q. Li, S. Xie, B. Zou, J. Appl. Phys. **93**, 9983 (2003)
27. C. Aydin, H.M. El-Nasser, F. Yakuphanoglu, I.S. Yahia, M. Aksoy, J. Alloy Comp. **509**, 854 (2011)
28. A.A.M. Farag, I.S. Yahia, Opt. Commun. **283**, 4310 (2010)
29. T.S. Moss, *Optical Process in Semiconductors* (Butter Worths, London, 1959)
30. P.P. Banerjee, Proc. IEEE **73**, 1859 (2005)
31. F. Abeles, *Optical Properties of Solids* (North-Holland Publishing Company, London, 1972)
32. F. Yakuphanoglu, M. Kandaz, M.N. Yaraşır, F.B. Şenkal, Physica B **393**, 235 (2007)
33. International Centre for Diffraction Data. JCDPS, PCPDFWIN, v. 2.3; 2002, No. 89–1397
34. N. Hongen, H. Sung Hong, K. Kee-Kahb, S. Eun Woo, K. Eui Jung, Materials Letters **63**, 2246 (2009)
35. B. Saha, S. Das, K.K. Chattopadhyay, Sol. Energy Mater. Sol. Cells **91**, 311 (2007)
36. F. Urbach, Phys. Rev. **92**, 1324 (1953)
37. T. Minami, T. Kakumu, Y. Takeda, Thin Solid Films **290–291**, 1 (1996)
38. E. Burstein, Phys. Rev. **93**, 632 (1954)
39. K. Tominaga, H. Fukumoto, K. Kondou, Y. Hayashi, K. Murai, T. Moriga, I. Nakabayashi, Vacuum **74**, 683 (2004)
40. O.A. Azim, M.M. Abdel-Aziz, I.S. Yahia, Appl. Surf. Sci. **255**, 4829 (2009)
41. M. DiDomenico, S.H. Wemple, J. Appl. Phys. **40**, 720 (1969)
42. F.E. Ghodsi, H. Absalan, Acta Phys. Polon. A **118**, 659 (2010)
43. S. Cho, J. Ma, Y. Kim, Y. Sun, G.K.L. Wong, J.B. Ketterson, Appl. Phys. Lett. **75**, 2761 (1999)
44. N. Ohashi, T. Sekiguchi, K. Aoyama, I. Sakaguchi, T. Tsurumi, H. Haneda, J. Appl. Phys. **91**, 3658 (2002)
45. K. Vanhausden, W.L. Warren, C.H. Seager, D.R. Tallant, J.A. Voigt, B.E. Gnade, J. Appl. Phys. **79**, 7983 (1996)
46. Z.Q. Chen, S. Yamamoto, M. Maekawa, A. Kawasuso, X.L. Yuan, T. Sekiguchi, J. Appl. Phys. **94**, 4807 (2003)